10. At 240°C, the highest temperature investigated, the pressure generated in these tubes amounted to only 33 atm, too low to produce a significant effect on the rates of known reactions in solution [for a survey, see W. J. le Noble, *Prog. Phys. Org. Chem.* **5**, 207 (1967)]. The sealed quartz tubes (1 cm in outside diameter, with a 2-mm wall) used in these experiments proved superior to sealed borosilicate tubes in strength and resistance to solvent attack. In addition, quartz tubes allowed the progress of decarboxylation of 1-methylorotate to be monitored without the opening of the tube, by observation of the ultraviolet absorption spectrum of the contents at intervals by means of a diode array spectrophotometer.
11. The absence of catalysis by methylamine is of special interest, in view of the fact that lysine is the single active site residue whose presence has been identified as essential for the catalytic activity of OMP decarboxylase [J. A. Smiley and M. E. Jones, *Biochemistry* **31**, 12162 (1992)].
12. This rate constant is smaller than a value extrapolated earlier (5×10^{-14} s^{-1}) for 1,3-dimethylorotic acid at 37°C from its behavior in sulfolane at 206° and 226°C (*6*). This difference in rates is probably due at least in part to differences in substrate structure.
13. K. J. Laidler, *Chemical Kinetics* (McGraw-Hill, New York, ed. 2, 1965), pp. 488–537.
14. Linear Arrhenius plots are almost invariably observed for simple chemical reactions (*13*), but departures from linearity have been reported occasionally for more complex physiological processes in which the mechanism or the rate-determining step changes with temperature [for a review, see F. H. Johnson, H. Eyring, M. J. Polissar, *The Kinetic Basis of Molecular Biology* (Wiley, New York, 1954), pp. 187–285]. In those few cases in which nonlinearity has been observed, the slope at lower temperature is greater than the slope at higher temperature. If the same were true of the simple reactions described here (an unlikely possibility that cannot be tested at present), then the rate of reaction at 25°C would have been overestimated by the present extrapolations.
15. P. W. Tucker, E. E. Hazen Jr., F. A. Cotton, *Mol. Cell. Biochem.* **22**, 67 (1978).
16. C. A. Bunton, M. M. Mhala, K. G. Oldham, C. A. Vernon, *J. Chem. Soc.* **1960**, 3293 (1960).
17. At temperatures above 100°C, hydrolysis of dimethylphosphate proceeds even more slowly than does decarboxylation of 1-methylorotic acid (Fig. 2). The entropy of activation for decarboxylation is positive (+19.7 cal deg^{-1} mol^{-1}), whereas that of phosphodiester hydrolysis is negative (−27.8 cal deg^{-1} mol^{-1}), so that decarboxylation proceeds much more slowly than does phosphodiester hydrolysis in neutral solution at room temperature. Values of these entropies of activation are in the ranges typically observed for mono- and bimolecular reactions, respectively (*13*).
18. E. H. Serpersu, D. Shortle, A. S. Mildvan, *Biochemistry* **25**, 68 (1986).
19. If there is a difference in mechanism between the enzymatic reaction and the nonenzymatic reaction or if the rate of the enzyme reaction is limited by some event that does not involve bond making or breaking in substrates, such as product release, then these values represent upper limits of the dissociation of the enzyme-substrate complex in the transition state [for a review, see R. Wolfenden, *Annu. Rev. Biophys. Bioeng.* **5**, 271 (1976)].
20. Table 1 is restricted to enzyme reactions that do not appear to proceed by double displacement mechanisms [D. E. Koshland Jr., *Biol. Rev. Camb. Philos. Soc.* **28**, 416 (1953)], because comparisons of enzymatic and nonenzymatic reaction rates do not permit straightforward estimation of transition state affinity for reactions of this type (*19*). Large rate enhancements, although not as large as that for OMP decarboxylase, have also been reported for certain multisubstrate reactions, including those catalyzed by catechol *O*-methyltransferase [I. Mihel, J. O. Knipe, J. K. Coward, R. L. Schowen, *J. Am. Chem. Soc.* **101**, 4349 (1979)] and lactate dehydrogenase [J. W. Burgner II and W. J. Ray, *Biochemistry* **23**, 3636 (1984)].
21. S. A. Acheson, J. B. Bell, M. E. Jones, R. Wolfenden, *Biochemistry* **29**, 3198 (1990).
22. J. A. Smiley, P. Paneth, M. H. O'Leary, J. B. Bell, M. E. Jones, *ibid.* **30**, 6216 (1991).
23. 5′-Phosphoribosylbarbituric acid, a competitive inhibitor with an inhibition constant value of $\sim 10^{-11}$ M, is bound noncovalently (*21*) 4 to 5 orders of magnitude more tightly than is the substrate or product, probably because of its resemblance to a nitrogen ylide intermediate in OMP decarboxylation [H. L. Levine, R. S. Brody, F. H. Westheimer, *ibid.* **19**, 4993 (1980)].
24. Auxotrophs of *Escherichia coli* have been used to prepare an antibody catalyzing the decarboxylation of orotic acid [J. A. Smiley and S. J. Benkovic, *Proc. Natl. Acad. Sci. U.S.A.* **91**, 8319 (1994)]. The present results indicate that this antibody achieves a remarkable catalytic proficiency of approximately 10^{15} M^{-1}, although yeast OMP decarboxylase exceeds that value by a factor of roughly 10^8.
25. E. R. Garrett and P. J. Mehta, *J. Am. Chem. Soc.* **94**, 8532 (1972).
26. D. P. Dumas, S. R. Caldwell, J. R. Wild, F. M. Raushel, *J. Biol. Chem.* **264**, 19659 (1989).
27. D. C. Hawkinson, T. C. M. Eames, R. M. Pollack, *Biochemistry* **30**, 10849 (1991).
28. A. Hall and J. R. Knowles, *ibid.* **14**, 4348 (1975).
29. E. H. Serpersu, D. Shortle, A. S. Mildvan, *ibid.* **25**, 68 (1986).
30. S. W. Hunt and P. A. Hoffee, *J. Biol. Chem.* **257**, 14240 (1982).
31. W. E. DeWolf Jr., F. A. Fullin, V. L. Schramm, *ibid.* **254**, 10868 (1979).
32. J. R. Whitaker, G. Menger, M. L. Bender, *Biochemistry* **5**, 386 (1986).
33. R. M. Pollack, B. Zeng, J. P. G. Mack, S. Eldin, *J. Am. Chem. Soc.* **111**, 6419 (1989).
34. S. J. Putman, *Biochem. J.* **129**, 301 (1972).
35. H. Steiner, B.-H. Jonsson, S. Lindskog, *Eur. J. Biochem.* **59**, 253 (1975).
36. J. L. Kofron, P. Kuzmic, V. Kishore, E. Colon-Bonilla, D. H. Rich, *Biochemistry* **30**, 6127 (1991).

37. Supported by NIH grant GM-18325. We are grateful to S. Rowley for technical assistance.

22 June 1994; accepted 29 September 1994

Structure-Based Design of Transcription Factors

Joel L. Pomerantz, Phillip A. Sharp, Carl O. Pabo

Computer modeling suggested that transcription factors with novel sequence specificities could be designed by combining known DNA binding domains. This structure-based strategy was tested by construction of a fusion protein, ZFHD1, that contained zinc fingers 1 and 2 from Zif268, a short polypeptide linker, and the homeodomain from Oct-1. The fusion protein bound optimally to a sequence containing adjacent homeodomain (TAATTA) and zinc finger (NGGGNG) subsites. When fused to an activation domain, ZFHD1 regulated promoter activity in vivo in a sequence-specific manner. Analysis of known protein-DNA complexes suggests that many other DNA binding proteins could be designed in a similar fashion.

Transcription factors are critical regulators of gene expression. The rational design of transcription factors with novel DNA binding specificities and regulatory activities will provide reagents for both biological research and gene therapy. The recent determination of a series of structures of protein-DNA complexes has facilitated a design strategy that uses computer modeling to predict how DNA binding domains could be combined to generate novel specificities. We explored this strategy by designing and testing a zinc finger–homeodomain fusion protein.

Computer modeling studies were used to visualize how zinc fingers might be fused to the Oct-1 homeodomain. The known crystal structures of the Zif268-DNA (*1*) and Oct-1–DNA (*2*) complexes were aligned by superimposition of the double helices in several different registers. Two arrangements were particularly interesting. In one alignment, the COOH-terminal end of zinc finger 2 was 8.8 Å away from the NH_2-terminal arm of the homeodomain (Fig. 1), which suggested that a short polypeptide linker could connect these domains. In this model, the fusion protein would bind a hybrid DNA site with the sequence 5′-AAATNNTGGGCG-3′. The Oct-1 homeodomain would recognize the AAAT subsite, zinc finger 2 would recognize the TGG subsite, and zinc finger 1 would recognize the GCG subsite. There was no possibility for steric interference between the zinc fingers and the homeodomain in this arrangement. Superimposition of the DNA duplexes in other registers generated a second plausible arrangement for a hybrid protein (*3*); however, this model was not as favorable because there was a risk of steric interference between the zinc fingers and the homeodomain.

The design strategy was tested by construction of a fusion protein, ZFHD1, that contained fingers 1 and 2 of Zif268, a gly-gly-arg-arg linker, and the Oct-1 homeodomain (Fig. 2A). A glutathione-S-transferase (GST) domain was added to facilitate expression and purification, and the DNA binding activity of this fusion protein was

J. L. Pomerantz, Center for Cancer Research, Department of Biology, and Harvard-MIT Division of Health Sciences and Technology, Massachusetts Institute of Technology, Cambridge, MA 02139, USA.
P. A. Sharp, Center for Cancer Research and Department of Biology, Massachusetts Institute of Technology, Cambridge, MA 02139, USA.
C. O. Pabo, Howard Hughes Medical Institute and Department of Biology, Massachusetts Institute of Technology, Cambridge, MA 02139, USA.

determined by selection of binding sites from a random pool of oligonucleotides. After four rounds of selection, 16 sites were cloned and sequenced (Fig. 2B). Comparison of these sequences revealed the consensus binding site 5′-TAATTANGGGNG-3′ (Fig. 2C). The 5′ half of this consensus, TAATTA, resembled a canonical homeodomain binding site (TAATNN) (*4*) and matched the site (TAATNA) that is preferred by the Oct-1 homeodomain in the absence of the POU-specific domain (*5*). The 3′ half of the consensus, NGGGNG, resembled adjacent binding sites for fingers 2 (TGG) and 1 (GCG) of Zif268. The guanine residues were more tightly conserved than were the other positions in these zinc finger subsites, and the crystal structure shows that these are the positions of the critical side-chain–base interactions (*1*).

The ZFHD1 consensus sequence (5′-TAATTANGGGNG-3′) matched the model that appeared to be most structurally feasible (*6*), but because of the internal symmetry of the TAATTA subsite, this sequence was also consistent with the homeodomain binding in another orientation (Fig. 2D; compare mode 1 and mode 2). This alternative arrangement, in which the critical TAAT is on the other strand and is directly juxtaposed with the zinc finger (TGGGCG) subsites, was considered unlikely because modeling had suggested that this arrangement required a linker to span >20 Å between the COOH-terminus of finger 2 and the NH_2-terminus of the homeodomain. To determine how the homeodomain bound to the TAATTA sequence in the 5′ half of the consensus, ZFHD1 was tested for binding to probes (5′-TAATGATGGGCG-3′ and 5′-TCATTATGGGCG-3′) designed to distinguish between these orientations. ZFHD1 bound to the 5′-TAATGATGGGCG-3′ probe with a dissociation constant of 8.4×10^{-10} M and preferred this probe to the 5′-TCATTATGGGCG-3′ probe by a factor of 33 (Fig. 3A; compare lanes 6 to 10 and 11 to

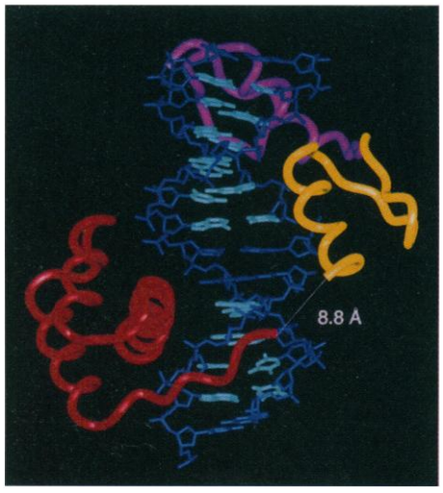

Fig. 1. Model of a zinc finger–homeodomain hybrid. Finger 1 of Zif268 is depicted in purple, finger 2 in yellow, and the Oct-1 homeodomain in red. The DNA is blue, with the base pairs in the AAAT and TGGGCG subsites highlighted in cyan; the hybrid protein recognizes a sequence of the form 5′-AAATNNTGGGCG-3′. The C_α of Gly^{59} (COOH-terminus of finger 2) is 8.8 Å from the C_α of Arg^2 (the first homeodomain residue visible in the crystal structure) (*18*). This figure was generated with Insight II (Biosym Technologies, San Diego, California).

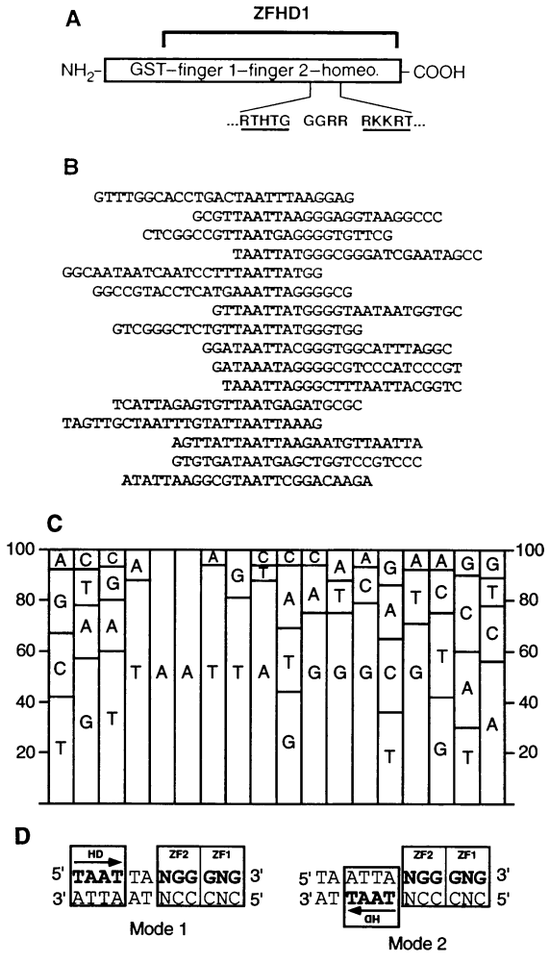

Fig. 2. Selection by ZFHD1 of a hybrid binding site from a pool of random oligonucleotides. (**A**) Structure of the fusion protein used to select binding sites (*19*). The underlined residues are from the Zif268-DNA (*1*) and Oct-1–DNA (*2*) crystal structures and correspond to the termini used in the computer modeling studies. The linker contains two glycine residues that were included for flexibility and the two arginine residues that are present at positions −1 and 1 of the Oct-1 homeodomain. (**B**) Sequences of 16 sites isolated after four rounds of binding site selection (*20*). (**C**) Consensogram derived from the sequences in (B) that indicates the percent occurrence of each nucleotide at each position. (**D**) Schematic diagram illustrating the two possible orientations of the homeodomain subsite relative to the zinc finger subsite suggested by the consensus. Mode 1 corresponds to the arrangement shown in Fig. 1.

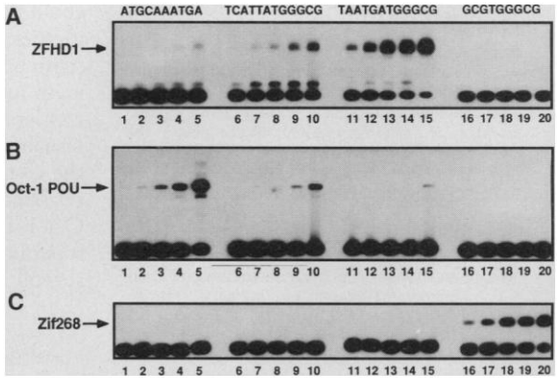

Fig. 3. Comparison of the DNA binding specificity of ZFHD1, the Oct-1 POU domain (which contains a homeodomain and a POU-specific domain), and the three zinc fingers from Zif268 (*21*). (**A**) The GST-ZFHD1 protein was titrated into DNA binding reactions containing the probe listed at the top of each set of lanes. Lanes 1, 6, 11, and 16 contain the protein at 9.8×10^{-11} M; protein concentration was increased in threefold increments in subsequent lanes of each set. The position of the protein-DNA complex is indicated by an arrow. (**B**) The PA–Oct-1 POU fusion protein (*16*) was titrated into parallel DNA binding reactions as in (A), but lanes 1, 6, 11, and 16 contain the protein at 2.1×10^{-12} M. The position of the protein-DNA complex is indicated by an arrow. (**C**) A peptide containing Zif268 fingers 1, 2, and 3 (*1*) was titrated into parallel DNA binding reactions, with lanes 1, 6, 11, and 16 containing the peptide at 3.3×10^{-11} M. The position of the protein-DNA complex is indicated by an arrow.

15). This suggested that the first four bases of the consensus sequence form the critical TAAT subsite that is recognized by the homeodomain (mode 1) and that ZFHD1 bound as predicted in the model (Fig. 1).

We compared ZFHD1, Oct-1, and Zif268 for their abilities to distinguish among the Oct-1 site 5′-ATGCAAATGA-3′, the Zif268 site 5′-GCGTGGGCG-3′, and the hybrid binding site 5′-TAATGATGGGCG-3′. The fusion protein ZFHD1 preferred the optimal hybrid site to the octamer site by a factor of 240 (Fig. 3A; compare lanes 1 to 5 and 11 to 15) and did not bind to the Zif site (lanes 16 to 20). The POU domain of Oct-1 (Fig. 3B) bound to the octamer site with a dissociation constant of 1.8×10^{-10} M (lanes 1 to 5), preferring this site to the hybrid sequences by factors of 10 (lanes 6 to 10) and 30 (lanes 11 to 15) and did not bind to the Zif site (lanes 16 to 20) (7). The three fingers of Zif268 (Fig. 3C) bound to the Zif site with a dissociation constant of 3.3×10^{-10} M (lanes 16 to 20) and did not bind to the other three sites (lanes 1 to 15). Thus ZFHD1 bound tightly and specifically to the hybrid site and displayed DNA binding specificity that was clearly distinct from that of either of the original proteins.

We fused ZFHD1 to a transcriptional activation domain and determined in transfection experiments whether the DNA binding protein could function in vivo. An expression plasmid encoding ZFHD1 fused to the COOH-terminal 81 amino acids of the herpes simplex virus VP16 protein (ZFHD1-VP16) was cotransfected into 293 cells with reporter constructs containing the SV40 promoter and the firefly luciferase gene. To determine whether the fusion protein could specifically regulate gene expression, we tested reporter constructs containing two tandem copies of the ZFHD1 site 5′-TAATGATGGGCG-3′, the octamer site 5′-ATGCAAATGA-3′, or the Zif site 5′-GCGTGGGCG-3′ inserted upstream of the SV40 promoter. When the reporter contained two copies of the ZFHD1 site, the ZFHD1-VP16 protein stimulated the activity of the promoter in a dose-dependent manner (8). Furthermore, the stimulatory activity was specific for the promoter containing the ZFHD1 binding sites (Fig. 4). At concentrations of protein that stimulated this promoter 44-fold, no stimulation above background was observed for promoters containing either the octamer or Zif sites. Thus, ZFHD1 efficiently and specifically recognized its target site in vivo.

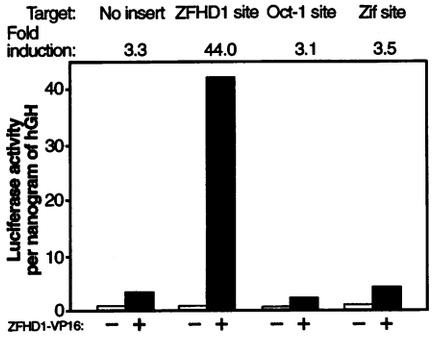

Fig. 4. Regulation of promoter activity in vivo by ZFHD1. The 293 cells were cotransfected with 5 μg of reporter vector, 10 μg of expression vector, and 5 μg of pCMV-hGH (gift of J. Parvin) used as an internal control (22). The reporter vectors contained two tandem copies of the ZFHD1 site (TAATGATGGGCG), the Oct-1 site (ATGCAAATGA), the Zif site (GCGTGGGCG), or no insert. The expression vector encoded the ZFHD1 protein fused to the COOH-terminal 81 amino acids of VP16 (plus signs), and the empty expression vector Rc/CMV was used as control (minus signs). The amount of luciferase activity obtained, normalized to hGH production, was set to 1.0 for the cotransfection of Rc/CMV with the no-insert reporter pGL2-Promoter. Bar graphs represent the average of three independent experiments. Actual values and standard deviation, reading from left to right, are: 1.00 ± 0.05, 3.30 ± 0.63; 0.96 ± 0.08, 42.2 ± 5.1; 0.76 ± 0.07, 2.36 ± 0.34; and 1.22 ± 0.10, 4.22 ± 1.41. Fold induction refers to the amount of normalized activity obtained with the ZFHD1-VP16 expression construct divided by that obtained with Rc/CMV.

This structure-based strategy of fusing known DNA binding modules may provide a general method for designing transcription factors with novel DNA binding specificities. Computer modeling suggests a number of other plausible arrangements for hybrid proteins. Figure 5 illustrates models of a zinc finger–basic-helix–loop-helix fusion protein (Fig. 5A) and a zinc finger–steroid receptor fusion protein (Fig. 5B) that should recognize hybrid binding sites. In each case, the modules can be fused by a short polypeptide linker without steric interference between the domains. This strategy could also be extended by variation in the length and sequence of the polypeptide linkers and then use of selection methods to optimize the binding affinity and specificity of the hybrid protein.

The strategy of fusing modules can also be combined with strategies for changing the sequence specificity of individual modules. Several DNA binding domains are amenable to mutational strategies for changing sequence specificity (9, 10), and zinc fingers may offer the most versatility (11). Combining structure-based design with mutational changes in specificity would greatly expand the range of sequences that could be targeted by hybrid domains.

The high affinity of ZFHD1 for its optimal site and the fact that ZFHD1, Oct-1, and Zif268 all clearly preferred different sites illustrate the success of the combinatorial approach. The specificity of the hybrid transcription factor depends on the relatively moderate affinity, but high sequence specificity, for the binding of a single module and on the chelate effect (12)

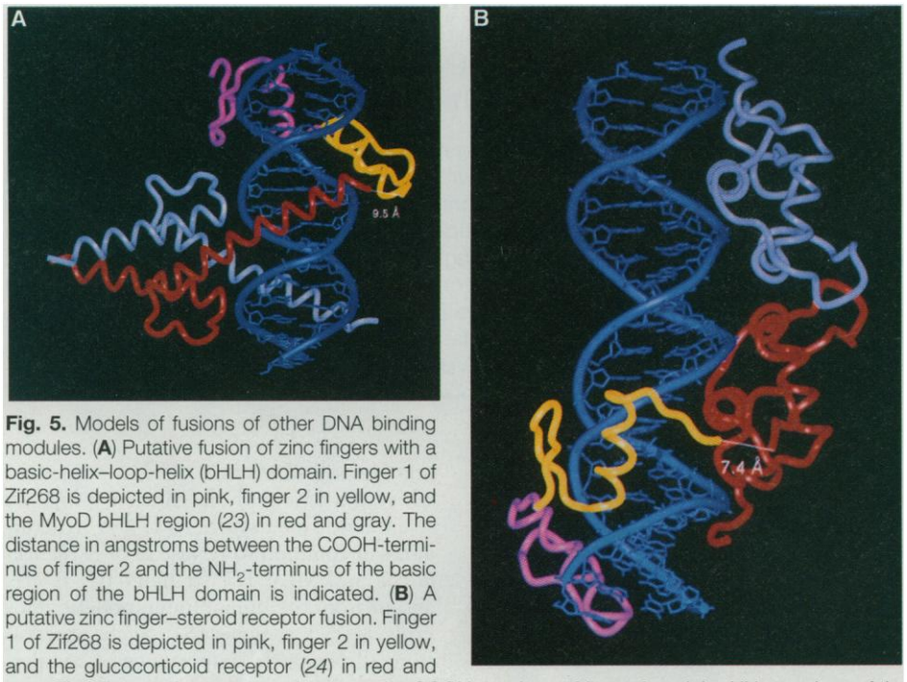

Fig. 5. Models of fusions of other DNA binding modules. (**A**) Putative fusion of zinc fingers with a basic-helix–loop-helix (bHLH) domain. Finger 1 of Zif268 is depicted in pink, finger 2 in yellow, and the MyoD bHLH region (23) in red and gray. The distance in angstroms between the COOH-terminus of finger 2 and the NH_2-terminus of the basic region of the bHLH domain is indicated. (**B**) A putative zinc finger–steroid receptor fusion. Finger 1 of Zif268 is depicted in pink, finger 2 in yellow, and the glucocorticoid receptor (24) in red and gray. The distance in angstroms between the COOH-terminus of finger 2 and the NH_2-terminus of the glucocorticoid receptor is indicated. These figures were generated with Insight II.

provided by the covalent linkage of modules. The design criteria that allowed the construction of ZFHD1 included the short length of polypeptide linker that was required to fuse the DNA binding domains and the absence of steric interference between these domains.

Designed transcription factors will be useful for the targeted regulation of specific cellular genes. The use of particular DNA binding domains in a hybrid (or the addition of other domains) may allow a protein to interact with other cellular factors or to be modulated by a particular regulatory pathway. The structure-based design of hybrid transcription factors should facilitate the development of efficient and specific reagents for biological research and gene therapy.

REFERENCES AND NOTES

1. N. P. Pavletich and C. O. Pabo, *Science* **252**, 809 (1991).
2. J. D. Klemm, M. A. Rould, R. Aurora, W. Herr, C. O. Pabo, *Cell* **77**, 21 (1994).
3. This alternative arrangement would also have a short (<10 Å) linker connecting zinc finger 2 to the homeodomain, but the subsites are arranged so that the predicted binding sequence is 5′-CGCCCANNAAAT-3′.
4. A. Laughon, *Biochemistry* **30**, 11357 (1991).
5. C. P. Verrijzer *et al.*, *EMBO J.* **11**, 4993 (1992).
6. No selected sites matched the binding sequence predicted for the alternative arrangement (*3*).
7. The relatively high affinity of the POU domain for the hybrid sites may result from nonspecific contacts made by the POU-specific domain.
8. J. L. Pomerantz, unpublished results.
9. P. Youderian, A. Vershon, S. Bouvier, R. T. Sauer, M. M. Susskind, *Cell* **35**, 777 (1983); R. P. Wharton and M. Ptashne, *Nature* **316**, 601 (1985); M. Suckow, A. Madan, B. Kisters-Wolke, B. von Wilcken-Bergmann, B. Muller-Hill, *Nucleic Acids Res.* **22**, 2198 (1994).
10. J. L. Pomerantz and P. A. Sharp, *Biochemistry* **33**, 10851 (1994).
11. E. J. Rebar and C. O. Pabo, *Science* **263**, 671 (1994); A. C. Jamieson, S.-H. Kim, J. A. Wells, *Biochemistry* **33**, 5689 (1994); R. Desjarlais and J. M. Berg, *Proc. Natl. Acad. Sci. U.S.A.* **90**, 2256 (1993).
12. W. P. Jencks, *Proc. Natl. Acad. Sci. U.S.A.* **78**, 4046 (1981).
13. B. A. Christy, L. F. Lau, D. Nathans, *ibid.* **85**, 7857 (1988).
14. R. A. Sturm, G. Das, W. Herr, *Genes Dev.* **2**, 1582 (1988).
15. F. M. Ausubel *et al.*, Eds., *Current Protocols in Molecular Biology* (Wiley, New York, 1994).
16. J. L. Pomerantz, T. M. Kristie, P. A. Sharp, *Genes Dev.* **6**, 2047 (1992).
17. P. E. Pellett, J. L. C. McKnight, F. J. Jenkins, B. Roizman, *Proc. Natl. Acad. Sci. U.S.A.* **82**, 5870 (1985).
18. Each model of a hybrid protein (Figs. 1 and 5) was constructed by juxtaposition of portions of two different crystallographically determined protein-DNA complexes. Models were initially prepared by superimposition of the double helices in various registers and were analyzed to see how the polypeptide chains might be connected. Superimposition of sets of phosphates typically gave root mean squared distances of 0.5 to 1.5 Å between corresponding atoms. These distances give some perspective on the error limits involved in modeling and were one of the reasons we chose a flexible linker containing several glycine residues for these initial studies.
19. A fragment encoding Zif268 residues 333 to 390 (*13*), two glycine residues, and Oct-1 residues 378 to 439 (*14*) was generated by polymerase chain reaction (PCR), confirmed by dideoxysequencing, and cloned into the Bam HI site of pGEX2T (Pharmacia) to generate an in-frame fusion to GST. The GST-ZFHD1 protein was expressed by standard methods (*15*), purified on glutathione Sepharose 4B (Pharmacia) according to the manufacturer's protocol, and stored at −80°C in 50 mM tris (pH 8.0), 100 mM KCl, and 10% glycerol. Protein concentration was determined by densitometric scanning of Coomassie-stained SDS–polyacrylamide gel electrophoresis (PAGE)–resolved proteins with the use of bovine serum albumin (BSA) (Boehringer Mannheim) as standard.
20. The probe used for random binding site selection contained the sequence 5′-GGCTGAGTCTGAACGGATCCN$_{25}$CCTCGAGACTGAGCGTCG-3′. Four rounds of selection were done as described (*10*), except that 100 ng of poly[d(I-C)]–poly[d(I-C)] and 0.025% NP-40 were included in the binding reactions. Selections used 5 ng of randomized DNA in the first round and approximately 1 ng in subsequent rounds. Binding reactions contained 6.4 ng of GST-ZFHD1 in round 1, 1.6 ng in round 2, 0.4 ng in round 3, and 0.1 ng in round 4.
21. DNA binding reactions contained 10 mM Hepes (pH 7.9), 0.5 mM EDTA, 50 mM KCl, 0.75 mM dithiothreitol, 4% Ficoll-400, and BSA (300 μg/ml), with the appropriate protein and binding site in a total volume of 10 μl. The concentration of binding site was always lower than the apparent dissociation constant by at least a factor of 10. The PA–Oct-1 POU fusion has been described (*16*). The purified three-finger Zif268 peptide (*1*) was a gift from M. Elrod-Erickson. Reactions were incubated at 30°C for 30 min and resolved in 4% nondenaturing polyacrylamide gels (*16*). Apparent dissociation constants were determined as described (*10*). Probes were derived by cloning of the following fragments into the Kpn I and Xho I sites of pBSKII+ (Stratagene) and excision of the fragments with Asp^{718} and Hind III: 5′-CCTCGAGGTCATTATGGGCGCTAGGTACC-3′, 5′-CCTCGAGGCGCCCATCATTACTAGGTACC-3′, 5′-CCTCGAGGCGCCCACGCCTAGGTACC-3′, and 5′-CCTCGAGGTCATTTGCATACTAGGTACC-3′.
22. The ZFHD1-VP16 expression vector was constructed by cloning of a fragment encoding the epitope Met-Tyr-Pro-Tyr-Asp-Val-Pro-Asp-Tyr-Ala, ZFHD1, and VP16 residues 399 to 479 (*17*) into the Not I and Apa I sites of Rc/CMV (Invitrogen). Reporter vectors were constructed by cloning of the following fragments into the Xho I and Kpn I sites of pGL2-Promoter (Promega): 5′-GGTACCAGTATGCAAATGACTGCAGTATGCAAATGACCTCGAG-3′, 5′-GGTACCAGGCGTGGGCGCTGCAGGCGTGGGCGCCTCGAG-3′, and 5′-GGTACCAGTAATGATGGGCGCTGCAGTAATGATGGGCGCCTCGAG-3′. The 293 cells were transfected with the use of calcium phosphate precipitation with a glycerol shock as described (*15*). Quantitation of human growth hormone (HGH) production was done with the Tandem-R HGH Immunoradiometric Assay (Hybritech, San Diego, CA) according to the manufacturer's instructions. Cell extracts were made 48 hours after transfection (*15*) and luciferase activity was determined with the use of 10 μl of 100 μl of total extract per 10-cm plate and 100 μl of Luciferase Assay Reagent (Promega) in a ML2250 Luminometer (Dynatech Laboratories, Chantilly, VA), with the use of the enhanced flash program and integration for 20 s with no delay.
23. P. C. M. Ma *et al.*, *Cell* **77**, 451 (1994).
24. B. F. Luisi *et al.*, *Nature* **352**, 497 (1991).

25. We thank J. Crispino, A. MacMillan, and J. Kim for critical reading of the manuscript; D. Shaywitz and J. Klemm for helpful discussions; members of the Sharp lab for their continual support; M. Siafaca for her ever-present assistance; L. Nekludova for help with modeling and programming; W. Xu and R. Sauer for help using Insight; and Y. Qiu and R. Issner for indispensable technical assistance. Supported by USPHS grant PO1-CA42063 from NIH, by cooperative agreement CDR-8803014 from NSF (to P.A.S.), and partially by the National Cancer Institute Cancer Center Support (core) grant P30-CA14051. Graphics were prepared with equipment purchased with support from the PEW Charitable Trusts and the Howard Hughes Medical Institute. C.O.P. is in the Howard Hughes Medical Institute. J.L.P. is partially supported by the Harvard Medical School M.D.-Ph.D. program.

9 September 1994; accepted 31 October 1994

Footprint Analysis of Replicating Murine Leukemia Virus Reverse Transcriptase

Birgitta M. Wöhrl, Millie M. Georgiadis, Alice Telesnitsky, Wayne A. Hendrickson, Stuart F. J. Le Grice*

Replication complexes that contained either murine leukemia virus reverse transcriptase (MLV RT) or a variant reverse transcriptase without a ribonuclease (RNase) H domain (ΔRH MLV RT) were visualized by enzymatic footprinting. Wild-type MLV RT protected template nucleotides +6 to −27, and primer nucleotides −1 to −26 of primers that had first been extended by one or four nucleotides. Although it catalyzed DNA synthesis, ΔRH MLV RT stably bound template-primer only under conditions of reduced ionic strength and protected the duplex portion only as far as position −15. Despite altered hydrolysis profiles, both enzymes covered primarily the template-primer duplex, contradicting recent predictions based on the structure of rat DNA polymerase β.

Even though they catalyze common reactions, retroviral reverse transcriptases (RTs) are structurally diverse. Whereas human, equine, feline, and simian enzymes share a heterodimeric organization of subunits encoded by the RT gene (*1–5*), a subunit of the avian sarcoma-leukosis virus (ASLV) enzyme retains the integrase domain of the gag-pol polyprotein (*6*). The isolated enzyme of the murine leukemia virus (MLV) is a 75-kD monomer, whereas a 150-kD homodimer is proposed to catalyze DNA synthesis (*7*). A structural motif common to RNase H of *Escherichia coli* and MLV RT (α helix III) is also absent from the human immunodeficiency virus (HIV) enzyme (*8*). Such observations illustrate the importance of comparative studies in understanding the evolution of these multifunctional enzymes.